Accuracy of tip-sample interaction measurements using dynamic atomic force microscopy techniques: Dependence on oscillation amplitude, interaction strength, and tip-sample distance

Omur E. Dagdeviren[1] and Udo D. Schwarz [1,2,*]

[1]Department of Mechanical Engineering and Materials Science, Yale University, New Haven, Connecticut 06520, USA

[2]Department of Chemical and Environmental Engineering, Yale University, New Haven, Connecticut 06520, USA

[*]Corresponding author: udo.schwarz@yale.edu

Abstract

Atomic force microscopy (AFM) is a versatile surface characterization method that can map a sample's topography with high spatial resolution while simultaneously interrogating its surface chemistry through the site-specific high-resolution quantification of the forces acting between the sample and the probe tip. Thanks to considerable advances in AFM measurement technology, such local measurements of chemical properties have gained much popularity in recent years. To this end, dynamic AFM methodologies are implemented where either the oscillation frequency or the oscillation amplitude and phase of the vibrating cantilever are recorded as a function of tip-sample distance and subsequently converted to reflect tip-sample forces or interaction potentials. Such conversion has, however, been shown to produce non-negligible errors when applying the most commonly used mathematical conversion procedures if oscillation amplitudes are of the order of the decay length of the interaction. Extending on these earlier findings, the computationally study presented in this paper reveals that the degree of divergence from actual values may also critically depend on both the overall strength of tip-sample interaction and the distance at which the interaction is obtained. These systematic errors can, however, be effectively eliminated by using oscillation amplitudes that are sufficiently larger than the decay length of the interaction potential.

Keywords: scanning probe microscopy/spectroscopy, atomic force microscopy, chemical interactions, tip-sample interactions, amplitude-modulation, frequency-modulation

I. Introduction

Atomic force microscopy (AFM) enables the mapping of a sample's topography through raster scanning a surface with a sharp tip, which can result in picometer spatial accuracy under optimal conditions.[1,2] Expanding from simple topography imaging, improvements in AFM methodologies made gauging the local tip-sample interaction potential and the force acting between the probe and the surface increasingly popular.[3,4] Initial measurements relied on measuring the deflection of a soft cantilever with a known spring constant that carries a sharp tip at the end once the tip has been brought into contact with the sample surface.[1,5-7] For such a setup, the contact area of the tip with the sample, which is typically much larger than a single-atom contact, determines the degree of locality of such measurements. In addition, mechanical instabilities inhibit positioning the tip in the vicinity of the sample surface where the gradient of the attractive surface forces becomes larger than the stiffness of the cantilever probe, preventing the measurement of short-ranged attractive chemical interactions.[3,8,9]

To overcome these limitations, 'dynamic' measurement schemes were introduced, where the tip is attached to the end of a cantilever that oscillates while the disturbance of the oscillation caused by the presence of the surface is measured to control the separation between the probe and the surface.[3,8] Implemented correctly, dynamic measurement schemes allow one to avoid tip instabilities and, as a consequence of the resulting improved vertical positional control, permit the prolonged use of tips terminated by a single atom, which promotes maximal locality of the measurement.[10] Two distinct approaches are commonly used: the amplitude-modulation (AM) technique, which is based on measuring the oscillation amplitude A and/or the phase difference between the oscillation and excitation ϕ while a constant excitation is applied,[8] and the frequency-modulation (FM) technique, which traces the change of resonance frequency Δf due to tip-sample interaction while keeping the oscillation amplitude constant.[3] Any of these two approaches enables the exploration of the chemical and electronic properties of the surface when performing so-called force spectroscopy experiments, which quantify the tip-sample interaction potential as a function of distance with up to picometer and piconewton resolution.[11-17] Historically, due to the lack of appropriate mathematical models, recovery of the interaction force was achieved indirectly: The recorded parameters were compared with numerically calculated frequency shifts or oscillation amplitudes/phases recursively until an agreement with the measured data was reached.[18,19] With

the subsequent development of appropriate mathematical reconstruction procedures, however, it became possible to obtain tip-sample interaction potentials (and, by calculating their derivative, ultimately forces) directly from the experimental data.[20-33]

Unfortunately, it has been found that when employing the most commonly applied recovery procedures, reconstructed force laws deviate non-negligibly from the actual values when the oscillation amplitude of the cantilever A is comparable to decay length of the tip-sample interaction l.[24,30,34,35] In an earlier study, we computationally and experimentally demonstrated that the deviations from the actual values can be eliminated by using oscillation amplitudes that are significantly larger than the decay length of the tip-sample interaction.[35] We also proposed an alternative force spectroscopy technique that relies on sweeping the oscillation amplitude up while keeping the base of the cantilever at a constant height from the surface, since this approach ensures accuracy in the relevant regimes for most interaction potentials while being simple and convenient to implement.[35] In this article, we show that the error likewise depends on the tip-sample separation and the strength of the interaction. Our numerical results also highlight that recovered interaction potentials may have misleading distance dependencies when the oscillation amplitude of the probe is comparable or smaller than the decay length of the interaction potential, which in particular inhibits determining the exact distance at which the potential energy reaches its minimum. Ultimately, our analysis establishes that oscillation amplitudes sufficiently larger than the decay length of the interaction potential must be used to effectively eliminate the systematic errors induced by mathematical reconstruction procedures.

II. Methods

In this section, we briefly summarize the computational methods for testing the accuracy of the interaction potentials reconstructed from measured data; for a more detailed description, please consult Ref. [35]. Our protocol starts with solving the equation of motion of a damped harmonic oscillator with external excitation and a non-linear tip-sample interaction force, which is a commonly used approach for dynamic AFM simulations:[9,18,28,33]

$$m\ddot{z}(t) + \frac{2\pi f_0 m}{Q}\dot{z}(t) + c_z[z(t) - d] = a_\mathrm{d} c_z \cos(2\pi f_\mathrm{d} t) + F_\mathrm{ts}[z(t), \dot{z}(t)] \ . \qquad (1)$$

Thereby, $z(t)$ is the position of the tip as a function of time t (with $z = d$ denoting the distance of the tip relative to the sample when the cantilever is undeflected); m, f_0, Q, and c_z are the effective

mass, the first eigenfrequency, the quality factor, and the spring constant of the oscillator, respectively. In Eq. (1), the terms on the left reflect the standard terms for a damped harmonic oscillator, while the first term on the right denotes the external excitation of the oscillator with excitation amplitude a_d and excitation frequency f_d. The second term on the right side symbolizes the non-linear tip sample interaction force F_{ts}, which may depend both on the tip's time-dependent position z as well as its instantaneous velocity $\dot{z}$. However, since a former study found the effect of a velocity-dependent component to be minimal for the range of oscillation amplitudes we use in our calculations,[35] we disregarded any velocity dependence and viscoelastic effects to decrease the computational cost. In agreement with previous literature,[9,28] we chose F_{ts} as a combination of a van der Waals-type sphere-over-flat interaction [36] for the attractive regime ($z \geq z_0$) and a contact force ($z < z_0$) that follows Maugis' approximation to the Derjaguin-Muller-Toporov model (DMT-M),[37-39] which is often referred to as Hertz-plus-offset model:[40]

$$F_{ts}(z) = \begin{cases} -\dfrac{A_H R}{6z^2} & \text{for } z \geq z_0 \\ \dfrac{4}{3} E^* \sqrt{R}\left(z_0 - z\right)^{3/2} - \dfrac{A_H R}{6 z_0^2} & \text{for } z < z_0 \end{cases}, \qquad (2)$$

where A_H = 0.2 aJ is the Hamaker constant, R = 10 nm the radius of the tip's apex, z_0 = 0.3 nm the distance at which the contact is established, and $E^* = ((1-\nu_t^2)/E_t + (1-\nu_s^2)/E_s)^{-1}$ the combined elastic modulus of the tip and sample (with E_t = 130 GPa as the Young's modulus of the tip, E_s = 1 GPa as the Young's modulus of the sample, and $\nu_t = \nu_s = 0.3$ as the Poisson ratios of tip and sample, respectively). The interaction force model Eq. (2) is usually considered a satisfying approximation for a realistic interaction of a probe tip with radius R with a generic flat surface and therefore regarded as a suitable choice when investigating the general operation characteristics of an atomic force microscope.[9,28,33,35] To systematically investigate the effect of the relative strength of the force on mathematical reconstruction procedures, we weighted the force law Eq. (2) calculated with these parameters with scaling factors between 0.01 and 2.0 to reflect the entire range of tip-sample interaction strengths that are typically encountered in high-resolution scanning probe microscopy experiments.[4] To describe the oscillating probe, we used c_z = 2,000 N/m and $f_d = f_0$ = 22,000 Hz; these values reflect typical parameters for a tuning fork glued on a holder in

qPlus configuration,[41] the currently most common oscillator choice for high-resolution, vacuum-based AFM.[3,42,43]

With all parameters and components defined, we calculated the frequency shift Δf for FM-type operation as a function of both the cantilever's oscillation amplitude A and the nearest tip-sample distance established during an individual oscillation cycle D by using a previously introduced analytical solution of Eq. (1) ;[9,35] note that D distinguishes itself from the distance d the tip has to the surface when the cantilever is undeflected by $D = d - A$. From the Δf data produced in this way, the tip-sample interaction potential $U_{ts}(D)$ can be recovered following the approach introduced by Sader and Jarvis, which represents the most widely used protocol for retrieving the tip-sample interaction potential.[24]

$$U_{\mathrm{ts}}(D) = 2c_z \int_D^{\infty} \frac{f_0 - f_{\mathrm{res}}}{f_0} \left[(z - D) + \sqrt{\frac{A}{16\pi}} \sqrt{z - D} + \frac{A^{3/2}}{\sqrt{2(z-D)}} \right] dz \, . \qquad (3)$$

In this equation, f_{res} stands for the cantilever's distance-dependent resonance frequency, i.e., $\Delta f = f_0 - f_{res}$. For the complementary comparison with AM-type force spectroscopy, we computed first the oscillation amplitude A and phase ϕ using the same analytic solution of Eq. (1), from which the tip-sample interaction potential U_{ts} can be obtained by solving:[28,30,32]

$$U_{\mathrm{ts}}(D) = 2c_z \int_D^{\infty} \frac{1}{2} \left[\frac{a_{\mathrm{d}}}{A} \cos\phi + \frac{f_0^2 - f_d^2}{f_0^2} \right] \left[(z - D) + \sqrt{\frac{A}{16\pi}} \sqrt{z - D} + \frac{A^{3/2}}{\sqrt{2(z-D)}} \right] dz \, . \qquad (4)$$

With the knowledge of $U_{ts}(D)$, the tip-sample force F_{ts} as a function of D can easily be generated for both cases by calculating its negative gradient ($F_{ts}(D) = -\partial U_{ts}/\partial D$).

III. Results

Force spectroscopy experiments are generally conducted with 'distance sweep' experiments where the cantilever base is moved relative to the sample surface while the response of the cantilever to the change in the tip-sample interaction is measured.[35] To start our analysis, we concentrate first on addressing the accuracy of FM-based force spectroscopy for a tuning fork with a quality factor of Q = 10,000. Following the approach described in the previous section, we calculated the frequency shift as a function of distance by solving Eq. (1) and then used Eq. (3) to recover the

tip-sample *force* for different oscillation amplitudes and different interaction strengths. Figure 1 illustrates two key findings:

(i) Comparing the reconstructed force laws for different oscillation amplitudes (solid colored lines) in the long-range regime (inset I) and the strongly attractive short-range part of the interaction (i.e., the segment of the curve just before the force minimum is reached; see inset II) with the original model force (dashed black line), we note that the deviation from the force law is inversely proportional to oscillation amplitude but less than 20 piconewton for all oscillation amplitudes.

(ii) In contrast, the error diverges for amplitudes $A < 1$ nm at distances smaller than the force minimum (see inset III). In this regime, the reconstructed force curves exhibit instabilities manifesting as erratic fluctuations of varying intensity with increasingly diverging errors, emphasized by a gradually more intense red background. For $A = 1$ nm, however, agreement between the model force and the recovered force is excellent even in the repulsive regime.

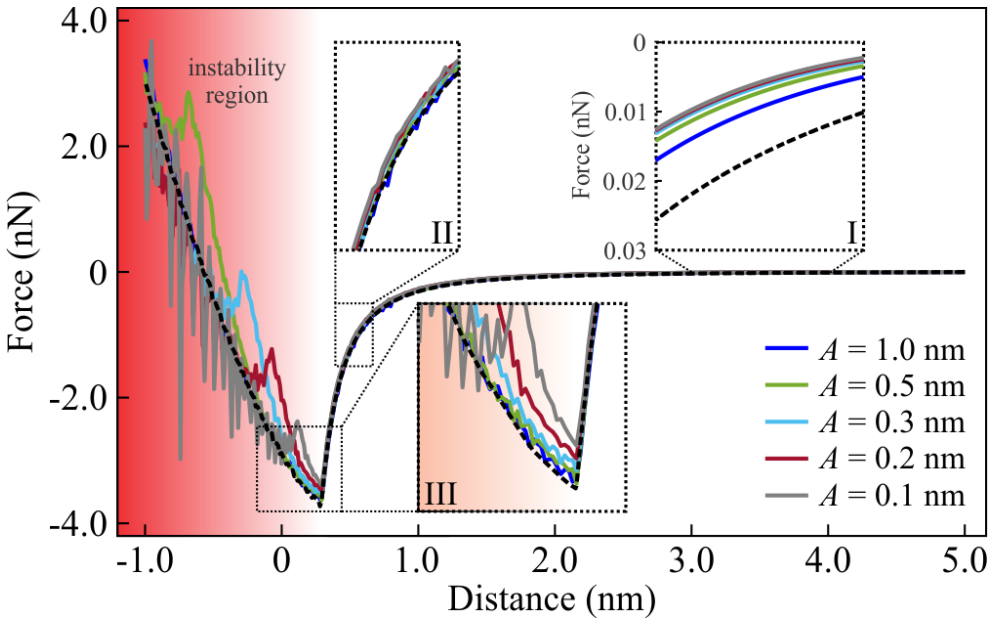

Figure 1: Example of force reconstruction from FM-based spectroscopy. With the dashed black curve depicting the original model force $F_{ts}(D)$ as defined in Eq. (2), noticeable discrepancies between the model force and the progression of the recovered curves are found for oscillation amplitudes A smaller than 1.0 nm. The error depends on tip-sample separation and inflates with decreasing tip-sample distance (marked by the red color gradient as "instability region"). For the calculations presented, we used typical values for a tuning fork in qPlus configuration under vacuum conditions, i.e., $c_z = 2000$ N/m, $f_0 = 22{,}000$ Hz, and $Q = 10{,}000$.

To further investigate the accuracy of the spectroscopy techniques under different scenarios, we also studied the distance-dependent error of the reconstructed tip-sample *potential* as a function of oscillation amplitude and interaction strength. Figure 2 shows as an example the case of FM-based spectroscopy for A = 0.3 nm and a scaling factor of 1. We can see that for these parameters, the reconstructed interaction potential (blue curve) deviates significantly from the model tip-sample interaction potential (dashed black curve) with the error evolving as a function of tip-sample separation and peaking around the potential energy minimum. In addition, features that when calculating the tip-sample interaction force by means of derivation give rise to the observed oscillations are also evident in the tip-sample interaction potential energy, such as the bump close to the energy minimum of the reconstructed tip-sample interaction potential (blue curve) in Figure 2. Close examination also reveals that the potential energy minimum of the reconstructed potential is located at a different distance than the model interaction potential, with the difference being denoted as ΔD.

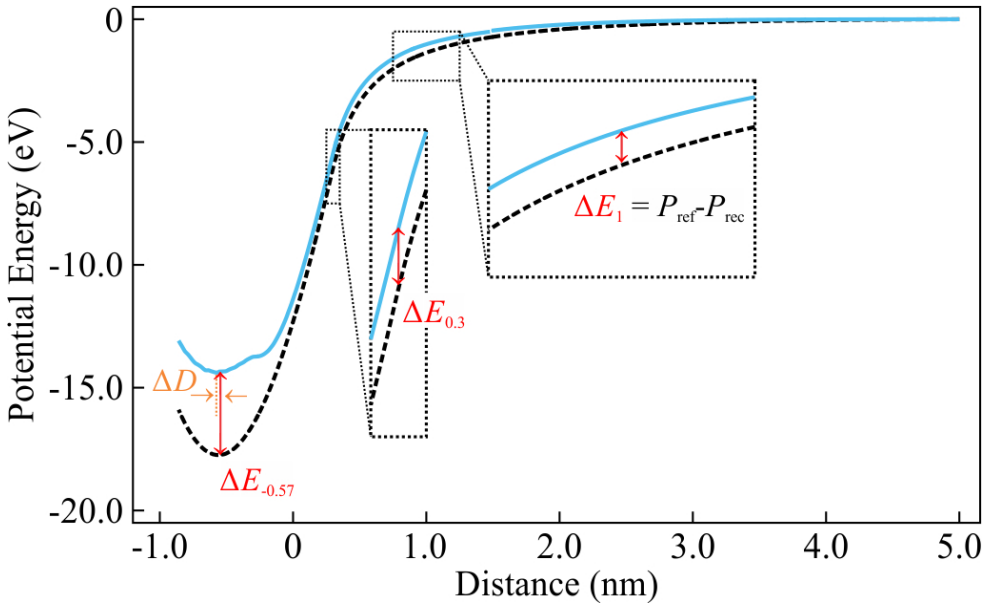

Figure 2: Figure illustrating the discrepancies in potential energy reconstruction that may occur when attempting to reconstruct the model potential $U_{\text{model}}(D)$ (dashed black curve) from FM spectroscopy data. Thereby, the solid blue curve was obtained setting A = 0.3 nm for a cantilever with the same characteristics as in Fig. 1 using the Sader-Jarvis approach Eq. (3).[44] Noticeable discrepancies between the model potential and the reconstructed potential emerge as a function of tip-sample separation. For further systematic investigations, we calculated the errors of each reconstructed interaction potential for three different tip-sample distances D = 1.0 nm (representing a long-ranged effect), 0.3 nm (i.e., at the force minimum as defined in Eq. (2)), and -0.57 nm (which matches the minimum of the model potential), which are referred to as ΔE_1, $\Delta E_{0.3}$, and $\Delta E_{-0.57}$, respectively, with $\Delta E = U_{\text{model}} - U_{\text{recovered}}$ (red double arrows). For additional

insight, we also calculated the difference ΔD between the minimum of the model potential, occurring at the location of $\Delta E_{-0.57}$, and the location of the minimum of the recovered curve (indicated by the faint orange line).

Moving now to a systematic screening, we calculated the errors ΔE_1 (long-range error), $\Delta E_{0.3}$ (error at model force minimum), and $\Delta E_{-0.57}$ (error at potential minimum) as defined in Fig. 2 for interaction potentials as well as their force equivalents ΔF_1, $\Delta F_{0.3}$, and $\Delta F_{-0.57}$ for a wide range of oscillation amplitudes (0.01 nm $\leq A \leq$ 3.0 nm) and scaling factors (0.01 $\leq$ *Scaling Factor* $\leq$ 2.0). The data is summarized in Fig. 3, where the errors are plotted color coded as a percentage of the original value. From panels (a) and (b), we can extract that for both reconstructed force and interaction potential, FM-based spectroscopy approximates the original values in the long-range interaction regime (i.e., $D \geq 1.0$ nm) well for all force models (accuracy better than 5% in all cases). Upon closer approach to the surface, however, the recovered values may deviate substantially from the values determined from the model force Eq. (2) (panels c - f). This is true in particular for oscillation amplitudes similar or smaller than the *decay length* of the tip-sample interaction l, which is defined as the distance difference between the location of the force minimum at ≈0.30 nm to the location where the force has diminished to 1/e (≈37%) of its maximum strength (at ≈0.52 nm), which results in a decay length l of roughly 0.22 nm for the specific model force of Eq. (2). Although we limit the maximum relative discrepancy covered by the color scale in Figure 3 to 30%, the actual error of the recovered forces may rise up to 500% around the potential energy minimum for small oscillation amplitudes ($A <$ 0.03 nm; see panel (e)). In this context, it is worth noting that the relative error in the reconstructed force is typically higher than the complementary error calculated for the potential as the force is obtained by the numerical derivative of the potential energy, which introduces the at times drastic fluctuations of the force visible in the red part of Fig. 1. Erratic fluctuations are also the reason why for the potential energy error at D = -0.57 nm (panel (f)) no clear trend can be pinpointed as a function of decreasing amplitude and calculating the error at slightly different distances (e.g., D = -0.47 nm or D = -0.67 nm) would similarly reveal seemingly uncorrelated trends. For oscillation amplitudes larger than 1.0 nm, however, both the reconstructed force and potential energy feature accuracies better than 5% for all scaling factors covered.

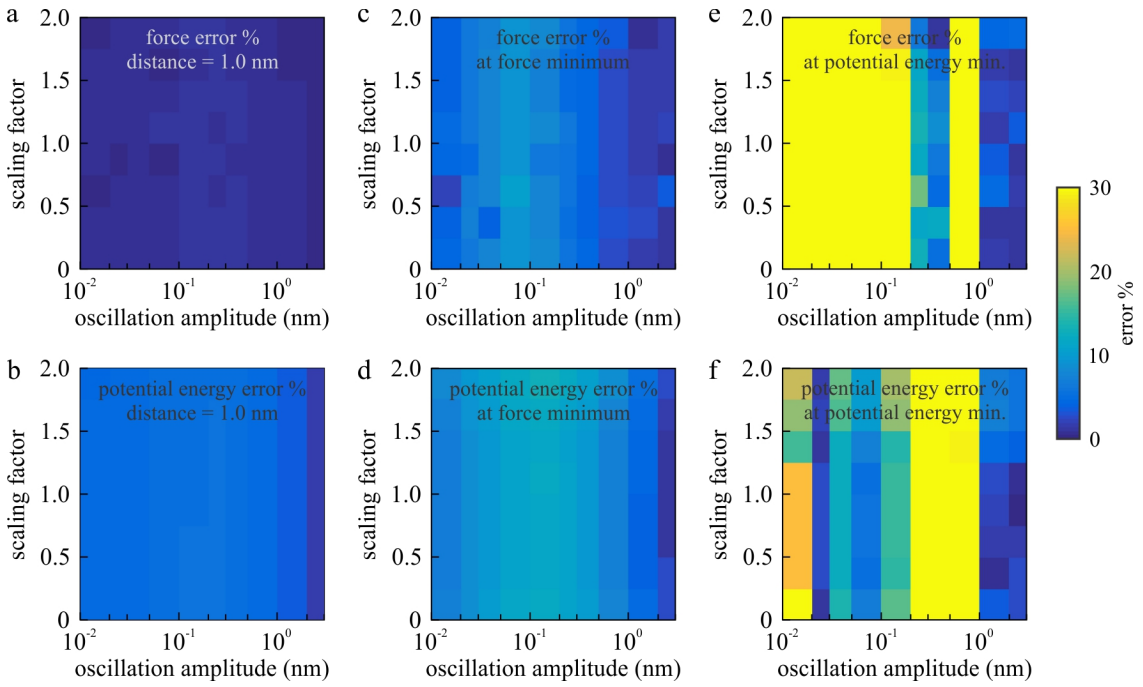

Figure 3: Analysis of the accuracy of force and potential energy reconstruction using FM-based spectroscopy as a function of scaling factor of the force model and the oscillation amplitude. The relative error of reconstructed force (a, c, e) and potential energy (b, d, f), reflected in percent of the original interaction strength by the color scale given in panel (a), was calculated at three different distances: values obtained for D = 1.0 nm provide insight into long-range accuracy (a, c); values obtained at D = 0.3 nm reflect reconstruction accuracy at the location of the minimum of the model force Eq. (2) (b, d), and values obtained at D = -0.57 nm reveal the ability of the mathematical conversion procedure employed for force reconstruction to correctly determine the equilibrium position of the tip-sample interaction (c, f). The error for both reconstructed force and potential energy diverges with decreasing distance. Parameters describing the cantilever (c_z, f_0, and Q) were kept the same as in Figs. 1 and 2.

With recent advances in AFM methodologies, force microscopy experiments can now also be conducted in ultra-high vacuum conditions with AM-based operation schemes when the oscillation of the probe is tuned electronically.[33] Due to the advantages that AM-based operation entails (in particular greater robustness and stability), we therefore also analyzed the accuracy of AM-based force spectroscopy for a tuning fork where the effective quality factor had been tuned to Q_{eff} = 300 while otherwise exhibiting our standard values for c_z and f_0. In this scenario, we additionally assumed the driving frequency f_d to match the resonance frequency of the free cantilever f_0 (i.e., $f_d = f_0$).[33] To this end, we calculated the *momentary oscillation amplitude A* and phase ϕ as a function of distance by solving Eq. (1) and then used Eq. (4) to recover the tip-sample force for different *free oscillation amplitudes* A_0 (i.e., the oscillation amplitudes the cantilever experiences far away from the surface; 0.01 nm $\leq A_0 \leq$ 3.0 nm) and scaling factors (0.01 $\leq$ *Scaling*

Factor ≤ 2.0) for the model interaction Eq. (2) and displayed the relative errors in Fig. 4 following the same protocol as in Fig. 3. Thereby, panels a and b demonstrate that AM-based force spectroscopy gives accurate force and potential energy values in the long-range interaction regime ($D \geq 1.0$ nm) for all interaction strengths and oscillation amplitudes, as did FM spectroscopy before. Mirroring the behavior already seen for FM spectroscopy, the errors for both potential energy and force increase for oscillation amplitudes comparable or smaller than the decay length of the tip-sample interaction l upon closer approach for the same reasons as previously discussed. Unlike the data from Fig. 3, however, we also observe a dependence of the error on the strength of the interaction, which is particularly well visible in panels (c) and (d). For oscillation amplitudes $A \geq 1.0$ nm, however, both the reconstructed force and potential energy exhibit an accuracy better than 5% within the distance range covered.

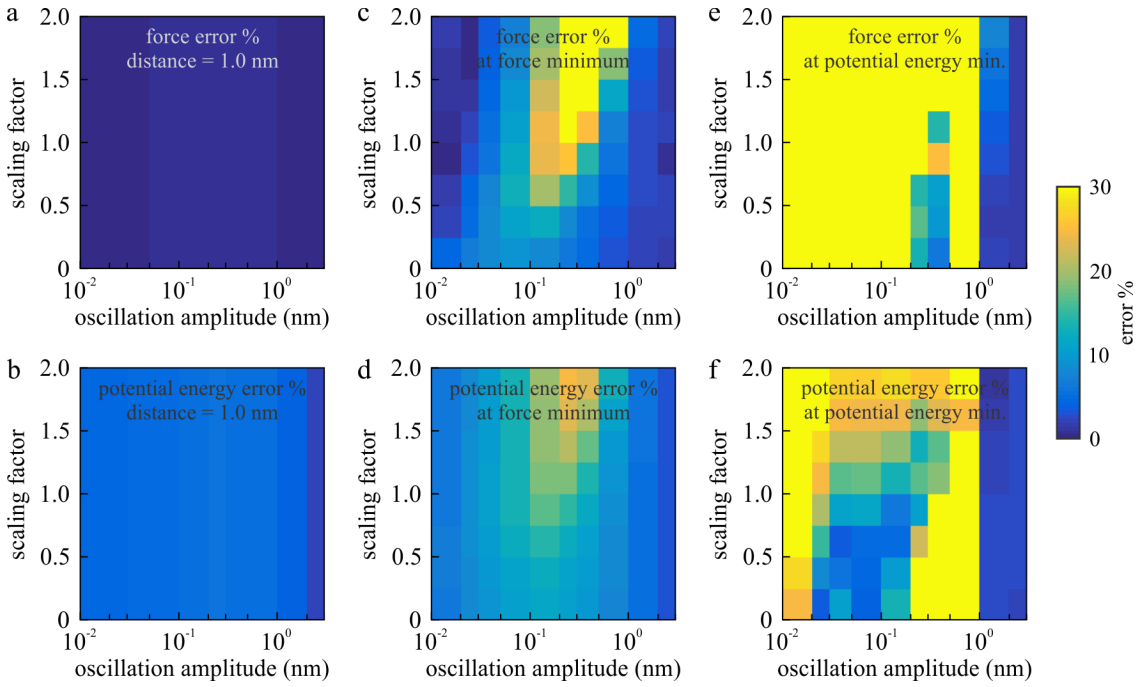

Figure 4: Analysis of the accuracy of force and potential energy reconstruction using AM-based spectroscopy as a function of scaling factor of the force model and the free oscillation amplitude A_0. Following the procedure employed in Fig. 3, we calculated the relative errors of reconstructed force (a, c, e) and potential energy (b, d, f) at D = 1.0 nm (a, b), 0.3 nm (c, d), and -0.57 nm (e, f). As with FM spectroscopy, the error for both the reconstructed force and the potential energy diverges with decreasing distance for all free oscillation amplitudes A_0 smaller than 1 nm. For the computations, we used a quality factor tuned to a value of $Q_{\text{eff}} = 300$ and assumed $f_d = f_0$ while keeping the other parameters consistent with our previous choices (i.e., $c_z = 2000$ N/m and $f_0 = 22{,}000$ Hz).

To complete our investigation, we calculated the absolute value of the difference between the distance at which the minimum of the reconstructed potential energy is found and the location of the actual potential energy minimum (represented as ΔD in Fig. 2) as a function of the same range of free oscillation amplitudes and interaction strength scaling factors covered above. For FM-based spectroscopy (Fig. 5a), the error is of the order of 1 Å for oscillation amplitudes smaller than 0.1 nm and is inert to the strength of the interaction. Notably, the error features a non-monotonic trend for oscillation amplitudes $A < 1$ nm due to the previously discussed fluctuating behavior of the reconstructed curves in the deep repulsive regime. Similarly, the error scales again with the strength of interaction for AM-based spectroscopy (Fig. 5b). In both cases, the error is negligibly small for oscillation amplitudes larger than 1.0 nm.

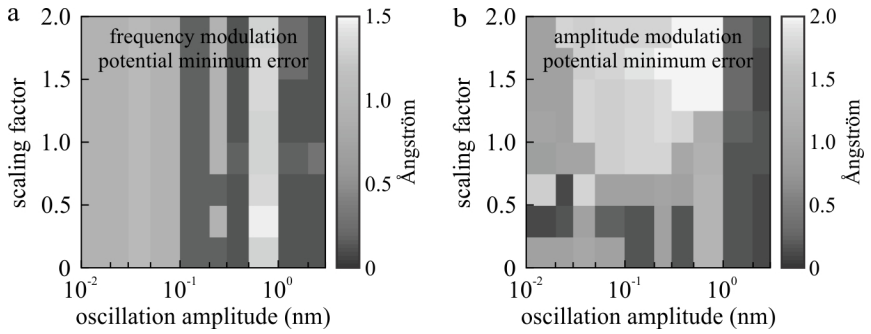

Figure 5: Analysis of the absolute error ΔD between the positions of the potential minima exhibited by the original model potential and the reconstructed potential (cf. Fig. 2) as a function of model potential's scaling factor and the free oscillation amplitude for FM (a) and AM (b) spectroscopy. In both cases, the error depends on the oscillation amplitude and can be >1 Å, but attenuates for free-oscillation amplitudes >1.0 nm. Interestingly, however, ΔD scales with interaction strength only for AM-based spectroscopy. For the calculations, we used the same parameters as previously in Figs. 3 and 4.

IV. Discussion

Summarizing the findings of Figure 3-5, we see that both FM- and AM-based spectroscopy reproduces the original tip-sample model well for free oscillation amplitudes A_0 that are much larger than the decay length of the attractive section of the interaction l. For both $A_0 \approx l$ and $A_0 << l$, however, the reconstructed force and potential curves can deviate considerably from the curve progression exhibited by the input model as defined in Eq. (2), which impedes quantitative characterization of chemical interactions. Although $A_0 \approx l$ is the most favorable imaging condition, our calculations show that it is a poor choice for spectroscopy experiments if accurate quantitative values are of importance. Moreover, we find that the error changes as a function of tip-sample separation, the magnitude of the attractive force, and the oscillation amplitude of the probe, but

that oscillation amplitudes larger than 1.0 nm reproduce the assumed model interactions with an error of less than 5%. This rule of thumb may, however, be re-assessed when measuring under substantially different circumstances such as, e.g., for data acquisition in liquids, where attractive interactions may be substantially suppressed compared to the case in vacuum, or when attempting to quantify electrostatic or magnetic forces, which are in comparison much more long-ranged than the surface forces characterized by Eq. (2).

The observed behavior can be explained by the influence of the nonlinear nature of the tip-sample interaction that induces a plethora of challenges for the correct recovery of the potential. Both Eqs. (3) and (4) are linear combinations of terms reflecting the 'small oscillation amplitude' case (i.e., $A_0 << l$), where an approximate solution can be derived assuming that the force changes linearly with the distance, and the 'large oscillation amplitude' case ($A_0 << l$), which has been obtained from perturbation theory. Both the small oscillation and large oscillation approximations work mostly well within their respective limits, even though we find that the small oscillation amplitude solution tends to erratically fluctuate within the deeply repulsive regime. To improve the accuracy of the transition region where $A_0 \approx l$, Sader and Jarvis introduced an additional term that was designed to be mathematically simple while still outcomes reproducible results, which was claimed to have a maximum discrepancy of 5% around the force minimum.[24] In recent work, we have shown that this is not always guaranteed and proposed as a work-around using either small or large oscillation amplitudes to actually achieve the promised accuracy. [35] This is in agreement with other work by Sader *et al*. (Ref. [34]) carried out in parallel to our previous study, which similarly concluded that if there is a fast-changing interacting potential, small or large oscillation amplitudes are ought to be used. Upon closer scrutiny, however, we can extract from inset I in Fig. 1 that for small oscillation amplitudes, there is still an appreciable error for small oscillation amplitudes even at 3.0 nm tip-sample separation despite being 'far' (as measured in units of the decay length l) from the region where the force is changing the most (located near the force curve's inflection point [34]). In addition, our numerical results show that to explore the progression of the potential energy curve around its minimum, using small oscillation amplitudes are not a solution due to the previously discussed erratic fluctuations, which cause the reconstructed values to have a divergent error up to 500% with respect to model interaction potential. We also observe that this discrepancy is more dominant for AM than for FM operation, possibly because for FM, only the relative motion of the resonance peak is important while for

AM the deformation of Lorentzian shape under the influence of tip-sample interaction enhances the error as the drive frequency is fixed around the free-resonance frequency of the oscillating probe. The same circumstances may also explain why the error scales with the maximum attractive force for AM spectroscopy but not for FM, as stronger interactions deform the shape of the resonance curve more than weaker do.

V. Conclusions

Recent advances in three-dimensional dynamic scanning force microscopy allow chemical interactions at and near the surface to be probed locally and quantitatively with picometer, piconewton, and milli-electron volt resolution. Towards this end, the local chemistry is tracked by tracing the force and potential energy acting between a sharp (ideally single-atom terminated) probe tip that is positioned with great accuracy in the proximity of the sample surface. We have now shown in this paper that the non-linear nature of tip-sample interaction may impose a systematic error into the mathematical procedures used to recover the tip-sample interaction, thereby limiting the accuracy in space and energy domains. Also, we have shown that the error in the recovered tip-sample interaction force and the error in the distance at which the force and potential energy minimums are measured evolves with the strength of the tip-sample interaction force. Our numerical calculations disclose that these systematic errors can be effectively eliminated by employing oscillation amplitudes that are sufficiently larger than the decay length of the tip-sample interaction potential.

Acknowledgments

As this method development directly benefits multiple projects, it has been equally supported by the National Science Foundation through grant CHE-1608568 and the Department of Energy through grant DE-SC0016179, which both provided funding for O. E. D.

References

[1] G. Binnig, C. F. Quate, and C. Gerber, Physical Review Letters **56**, 930 (1986).
[2] F. J. Giessibl, Science **267**, 68 (1995).
[3] F. J. Giessibl, Reviews of Modern Physics **75**, 949 (2003).
[4] D. A. Bonnell, D. N. Basov, M. Bode, U. Diebold, S. V. Kalinin, V. Madhavan, L. Novotny, M. Salmeron, U. D. Schwarz, and P. S. Weiss, Reviews of Modern Physics **84**, 1343 (2012).

[5] G. Binnig, G. Ch, E. Stoll, T. R. Albrecht, and C. F. Quate, EPL (Europhysics Letters) **3**, 1281 (1987).
[6] N. A. Burnham, R. J. Colton, and H. M. Pollock, Nanotechnology **4**, 64 (1993).
[7] S. Yongho and J. Wonho, Reports on Progress in Physics **71**, 016101 (2008).
[8] R. Garcia, *Amplitude Modulation Atomic Force Microscopy*. (Wiley-VCH, Singapore, 2010).
[9] H. Hölscher and U. D. Schwarz, International Journal of Non-Linear Mechanics **42**, 608 (2007).
[10] T. R. Albrecht, P. Grutter, D. Horne, and D. Rugar, Journal of Applied Physics **69**, (1991).
[11] L. Gross, F. Mohn, N. Moll, P. Liljeroth, and G. Meyer, Science **325**, 1110 (2009).
[12] L. Gross, F. Mohn, P. Liljeroth, J. Repp, F. J. Giessibl, and G. Meyer, Science **324**, 1428 (2009).
[13] B. J. Albers, T. C. Schwendemann, M. Z. Baykara, N. Pilet, M. Liebmann, E. I. Altman, and U. D. Schwarz, Nat Nano **4**, 307 (2009).
[14] M. Ondráček, P. Pou, V. Rozsíval, C. González, P. Jelínek, and R. Pérez, Physical Review Letters **106**, 176101 (2011).
[15] M. Ondráček, C. González, and P. Jelínek, Journal of Physics: Condensed Matter **24**, 084003 (2012).
[16] S. Bartosz, T. Glatzel, S. Kawai, Ernst M., R. Turansky, J. Brndiar, and I. Štich, Nanotechnology **23**, 045705 (2012).
[17] O. E. Dagdeviren, J. Götzen, E. I. Altman, and U. D. Schwarz, Nanotechnology **27**, 485708 (2016).
[18] B. Anczykowski, D. Krüger, K. L. Babcock, and H. Fuchs, Ultramicroscopy **66**, 251 (1996).
[19] B. Gotsmann, B. Anczykowski, C. Seidel, and H. Fuchs, Applied Surface Science **140**, 314 (1999).
[20] F. J. Giessibl, Physical Review B **56**, 16010 (1997).
[21] H. Hölscher, W. Allers, U. D. Schwarz, A. Schwarz, and R. Wiesendanger, Physical Review Letters **83**, 4780 (1999).
[22] U. Dürig, Applied Physics Letters **75**, 433 (1999).
[23] F. J. Giessibl, Applied Physics Letters **78**, 123 (2001).
[24] J. E. Sader and S. P. Jarvis, Applied Physics Letters **84**, 1801 (2004).
[25] E. S. John, U. Takayuki, J. H. Michael, F. Alan, N. Yoshikazu, and P. J. Suzanne, Nanotechnology **16**, S94 (2005).
[26] J. E. Sader and S. P. Jarvis, Physical Review B **74**, 195424 (2006).
[27] M. Lee and W. Jhe, Physical Review Letters **97**, 036104 (2006).
[28] H. Hölscher, Journal of Applied Physics **103**, 064317 (2008).
[29] H. Shuiqing and R. Arvind, Nanotechnology **19**, 375704 (2008).
[30] A. J. Katan, M. H. van Es, and T. H. Oosterkamp, Nanotechnology **20**, 165703 (2009).
[31] D. Platz, D. Forchheimer, E. A. Tholén, and D. B. Haviland, Nature Communications **4**, 1360 (2013).
[32] F. P. Amir, M.-J. Daniel, and G. Ricardo, Nanotechnology **26**, 185706 (2015).
[33] O. E. Dagdeviren, J. Götzen, H. Hölscher, E. I. Altman, and U. D. Schwarz, Nanotechnology **27**, 065703 (2016).
[34] J. E. Sader, B. D. Hughes, F. Huber, and F. J. Giessibl, in *arXiv:1709.07571* (2017).
[35] O. E. Dagdeviren, C. Zhou, E. I. Altman, and U. D. Schwarz, Physical Review Applied **9**, 044040 (2018).
[36] J. Israelachvili, *Intermolecular and Surface Forces*, 2 ed. (Academic Press, London, 1991).
[37] U. D. Schwarz, Journal of Colloid and Interface Science **261**, 99 (2003).
[38] D. Maugis and B. Gauthier-Manuel, Journal of Adhesion Science and Technology **8**, 1311 (1994).
[39] J. A. Greenwood and K. L. Johnson, Journal of Physics D: Applied Physics **31**, 3279 (1998).
[40] U. D. Schwarz, O. Zwörner, P. Köster, and R. Wiesendanger, Physical Review B **56**, 6987 (1997).
[41] F. J. Giessibl, Applied Physics Letters **73**, 3956 (1998).
[42] O. E. Dagdeviren and U. D. Schwarz, Measurement Science and Technology **28**, 015102 (2017).
[43] O. E. Dagdeviren and U. D. Schwarz, Beilstein Journal of Nanotechnology **8**, 657 (2017).
[44] J. E. Sader, Journal of Applied Physics **84**, 64 (1998).